Effect of Blend Rheology on the Transport Property of Oriented Poly(ethylene terephthalate) Blends

RAJAGOPALAN GOPALAKRISHNAN,[1] JEROLD M. SCHULTZ,[1,*] and RAMESH M. GOHIL[2]

[1]Materials Science Program, University of Delaware, Newark, Delaware 19716; [2]Circleville Research Laboratory, E. I. Du Pont de Nemours and Company, Circleville, Ohio 43113

SYNOPSIS

Rheological studies were performed to delineate appropriate stretching windows, and poly(ethylene terephthalate)/poly(ethylene-co-vinyl alcohol) blend films were extruded biaxially within such processing windows. The morphology and oxygen permeability properties of these films, with and without a compatibilizer, were characterized. The intent of this study was to achieve a blend oxygen permeability value (OPV) of less than 1. At a fixed draw ratio and draw temperature, appropriate rheological matching could lead to an increase in the aspect ratio of the EVOH phase and, thereby, of oxygen barrier properties. This study concludes that by melt viscosity matching it is not possible to obtain blends with OPV of less than 1. The model of Fricke, used to predict blend permeability, was found to be more accurate at the higher draw temperatures, with the measured values deviating increasingly negatively from the predicted values as the draw temperature is decreased. © 1995 John Wiley & Sons, Inc.

INTRODUCTION

Immiscible blends[1-4] of poly(ethylene terephthalate) (PET) are coming into increasing prominence. In the area of food packaging, the challenges posed by industry have necessitated the need for films with superior barrier properties.[5] In the past years, research efforts have been concentrated in this area to prepare packaging-quality films by using a variety of processing techniques.[1,6-10]

EVOH is one key polymer used in high gas barrier applications. It is resistant to the permeation of oxygen, carbon dioxide, other gases, and hydrocarbons. The main pitfalls of EVOH are its moisture sensitivity and its reduced oxygen permeability resistance with increasing relative humidity.[11] This problem is usually circumvented by coextruding in the form of laminates. However, since coextrusion involves large capital investments in addition to difficult process control, blending may be a cost-effective alternative. Coextrusion also involves the use of an adhesive since EVOH does not adhere to PET. EVOH can be blended with PET, EVOH being the minor, dispersed phase. In blending PET with EVOH, it is necessary to avoid degradation and crosslinking of EVOH. Good barrier properties can be obtained, provided that the rheological, morphological, and interfacial criteria are satisfied.

In this article, we study the effects of matching the rheological behavior of the matrix PET and the dispersed EVOH phase and the interfacial modification on the barrier properties of these blends. Previous studies have established that the phase morphology determines, to a large extent, the transport properties of the blend. In the case of immiscible blends where the second phase appears as distinct particles, a necessary requirement to obtain good barrier properties is that of a high aspect ratio of the dispersed phase.[6,12,13] Two crucial material parameters that control the blend morphology (and, hence, the aspect ratio) are the viscosities of the blend components and the interfacial adhesion[14,15] between the phases. On the processing side, the blend morphology is also sensitive to an orientation operation. Factors of importance here are the mode and extent (draw ratio) of orientation and the temperature of drawing.

For immiscible blends, maximum deformation in the second phase during orientation should be achieved when the viscosity ratio, λ, of the blend

Table I **Properties of the PET and EVOH Grades Used in This Study**

	PET				
Property	Selar PT 8202	Selar PT 8307	Selar PT 8257	Selar PT 3974	Shell PET
Intrinsic viscosity[a]	0.68	0.71	0.85	0.69	0.59
Glass transition Temperature	73°C	70°C	74°C	75°C	74°C
Melting point	230°C	220°C	231°C	231°C	256°C
Density	1.33 g/cc	1.33 g/cc	1.33 g/cc	1.33 g/cc	1.33 g/cc
OPV at 30°C, 80% RH[b]	9.6	8.3	9.6	9.6	3.8[c]

	EVOH				
Property	Units	Selar OH 4416	Selar OH 3003	BX 230	EVAL F	Soarnol D
Ethylene content	mol %	44	32	32	32	29
Density	g/cc	1.15	1.2	1.2	1.19	1.21
Melt flow at 210°C, 2.16 kg	g/10 min	12	3	1.6	3.1	8
Melting point	°C	168	183	183	181	188
OPV[d]						
At 20°C, dry		0.03			0.0066	0.012
At 30°C, dry		0.14	0.02	0.02	0.02	
At 30°C, 80% RH		0.33	0.12	0.12	0.046	0.041

[a] Measured in 50/50 methylene chloride/trifluoroacetic acid, 0.1 g/25 cc, 30°C.
[b] In cc/mil/100 sq in./day/atm.
[c] Permeability when oriented.
[d] Oxygen permeability value (OPV) is in cc/mil/100 sq in./day/atm.

components is close to unity.[16] Matching of viscosities should also lead to a finer dispersion after extrusion. In general, high or low viscosity ratios result in a coarse morphology. Avgeropoulos et al.,[17] in their work with (ethylene–propylene–diene monomer)/(polybutadiene rubber) blends, showed that small second-phase domains are obtained when the mixing viscosities of the two phases are about equal. Their findings also show that the particle size increases as the viscosity ratio is increased, since the shear stresses induced during deformation are not sufficient to break the dispersed domains at higher viscosity ratios. Wu[18] observed that the dispersed particles become larger as the viscosity ratio increases above unity or decreases below unity.

Another consideration in blend systems is that of modifying the PET–EVOH interface to achieve greater compatibilization. This will ensure a more efficient transfer of shear stresses from matrix to inclusion during extrusion and subsequent drawing and, consequently, led to more deformation of the EVOH phase. Further, addition of a compatibilizer should lead to a decrease in phase size since the interfacial tension is reduced. In this work, the effect of a compatibilizer (KRATON® FG-1901X) has been studied.

EXPERIMENTAL

Materials

The properties of the materials used in this study are given in Table I.

PET

Five PET grades were used in this work. Four of the grades were DuPont Selar®PT copolymer grades (viz., 8202, 8257, 8307, and 3974) of proprietary compositions with varying amounts of isophthalic acid and the fifth grade was the Shell TRAYTUF® 5900C homopolymer grade.

EVOH

The grades of EVOH used were DuPont Selar® OH BX 230, 3007, and 4416, EVAL F, and Nippon-Gohsei Soarnol D.

Table II Blends Prepared in This Work Through the Matching of the Flow Stresses of the PET and EVOH Grades

Blend No.	Composition PET/EVOH
1	3974/4416
2	3974/4416/compatibilizer
3	8257/3003
4	8257/3003/compatibilizer
5	Shell PET/4416
6	Shell PET/4416/compatibilizer
7	8202/3003
8	8202/3003/compatibilizer
9	8257/BX230
10	8257/BX230/compatibilizer
11	8202/BX230
12	8202/BX230/compatibilizer

All PET grades are Selar® PT grades. All EVOH grades, mentioned above, are Selar® OH grades. Compatibilizer used was KRATON® FG1901X, added 1% by weight. Other blends made were 8307/EVAL-F, uncompatibilized and compatibilized, and 8307/Soarnol-D, uncompatibilized and compatibilized.

Compatibilizer

The compatibilizer used was KRATON® FG-1901X, supplied by the Shell Chemical Co. It is a styrene–ethylene–butylene–styrene block copolymer (SEBS) with 2% grafted maleic anhydride.

Extrusion

The PET and EVOH grades were dried overnight in a dehumidified air oven at 120 and 80°C, respec-

tively. Extrusion was of two parts: In the first part, sheets of the pure homopolymer were extruded, and these sheets were then used for mechanical testing in the temperature range of 75–110°C. Based on the data obtained, blends were matched on a rheological basis, by matching the flow stresses in that temperature window. The blend combinations arrived at are given in Table II.

The blends were extruded using a 1.1-in. diameter W.P. twin-screw extruder through a 10-in. die and cast onto a rotating chill roll. The nominal thickness of the films was 20 mil. The extrusion temperatures used varied in the range 250–280°C, and the chill roll temperature varied from 50 to 60°C. Compatibilized blends were made by adding 1 wt % of the compatibilizer to the preblend mixture before extrusion.

Mechanical Testing

Tensile tests of as-cast film samples were done as per ASTM D882-88, using Test Method A.

Stretching

As-cast blends were stretched in an equal biaxial simultaneous mode using a T. M. Long laboratory stretcher. Samples of 11.25 cm were cut and films were soaked at the processing temperature for 2 min in the preheated stretching chamber and then stretched to a draw ratio of 3.5 × 3.5. The films were drawn at a stretch rate of 4500% per minute. Stretching temperatures used were 75, 80, 85, 90,

Table III Flow Stresses of the Unmodified Polymers

Grade of Homopolymer	Flow Stress (MPa)					
	70°C	80°C	90°C	100°C	110°C	120°C
PET						
Selar PT 8257	18.4	3.01	Not done	0.34	0.246	Not done
Selar PT 3974	14.43	2.54	Not done	0.33	0.115	Not done
Shell TRAYTUF	16.16	2.39	Not done	0.253	0.0703	Not done
Selar PT 8202	17.22	12.4	Not done	8.41	5.52	Not done
EVOH						
Selar OH 3003	21.52	15	Not done	9.67	Not done	6.93
Selar OH 4416	11.7	8.34	Not done	6.44	Not done	4.76
Soarnol-D	Not done	16.36	12.03	10.94	9.36	Not done
Soarnol-DT	Not done	14.81	11.46	9.72	8.52	Not done
Eval-F	Not done	14.28	12.77	10.06	7.74	Not done

The resin BX230 has a comparable viscosity to that of Selar OH 3003 and was blended accordingly. The viscosity properties of Selar PT 8307 are comparable to those of Selar PT 8257.
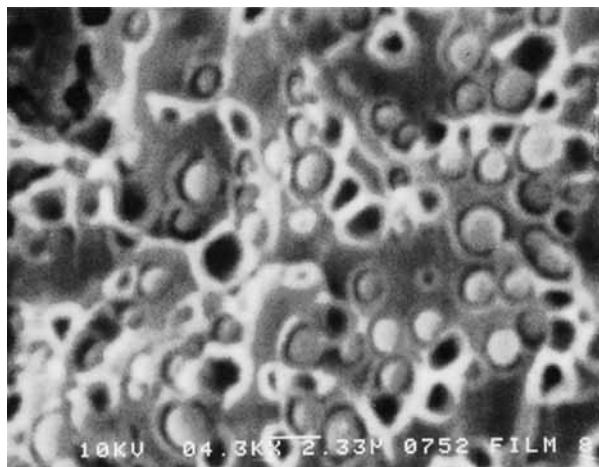
Figure 1 A representative fractograph of an as-cast blend.

and 110°C. After drawing, the films were allowed to cool before being removed from the grips. All drawn films were annealed while being constrained between metal frames, at 200°C for 3 min.

Permeability

Oxygen permeability values were measured using a Mocon Oxtran Twin oxygen permeability tester with a DL 200 data logger. The details of the procedure are summarized in Ref. 19. All readings were taken after the detector output remained unchanged for 6 min. All tests were done at 30°C and at a relative humidity of 80%.

Morphology

Blend films were cryogenically fractured either by bending or by puncturing. The fractured films were
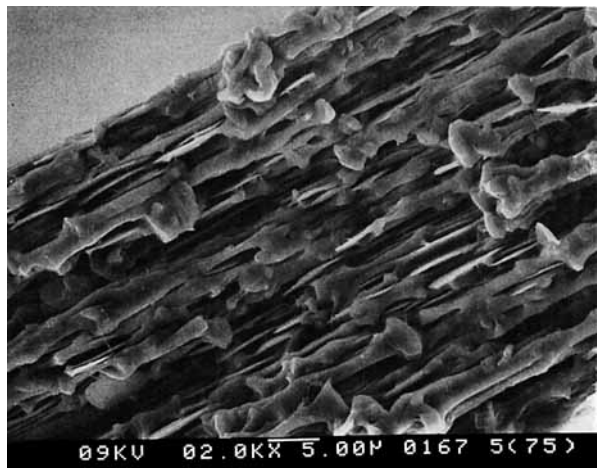
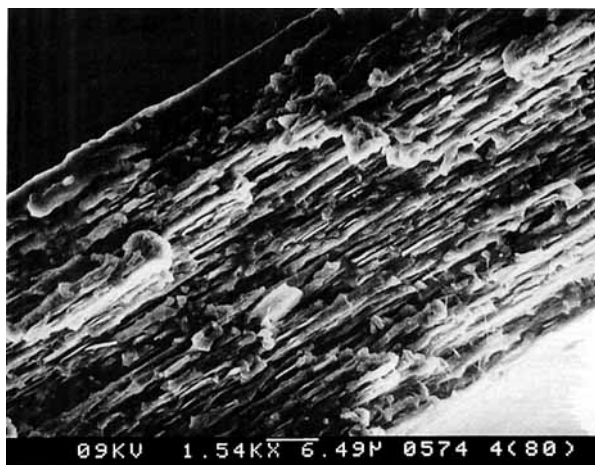**Figure 2** A representative fractograph of blends drawn at 75°C.

Figure 3 A representative fractograph of blends drawn at 80°C.

cut and mounted and the fracture surfaces were sputter-coated with gold and observed in an SEM. Microscopy was done on an ISI WB-6 SEM, at an accelerating voltage of 9 kV.

Thermal Characterization

Thermal characterization was performed using a DuPont 9900 DSC apparatus. A heating rate of 20°C/min was used in all tests.

RESULTS

Mechanical Testing

Table III shows the flow stresses vs. temperature for the homopolymers tested. Flow stresses for the
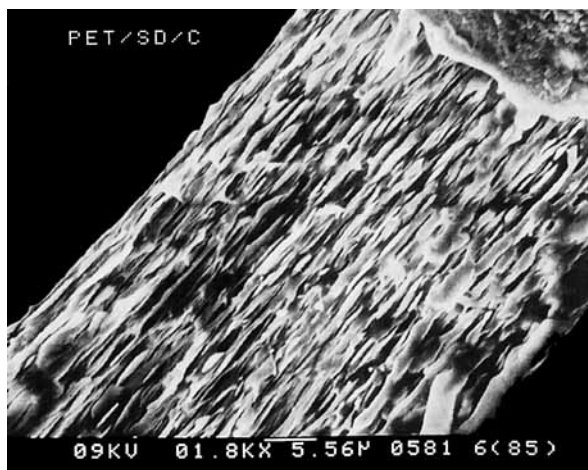

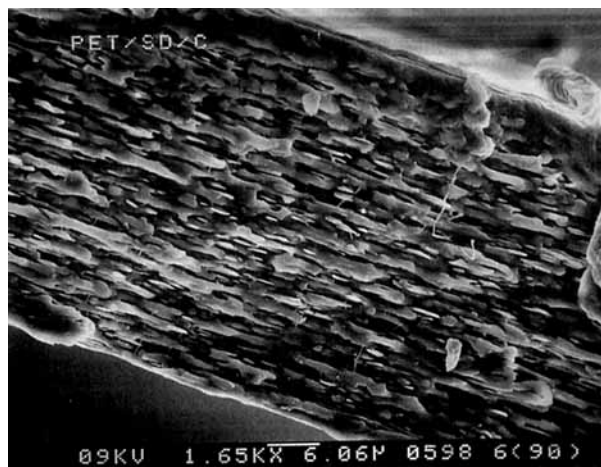**Figure 4** A representative fractograph of blends drawn at 85°C.

Figure 5 A representative fractograph of blends drawn at 90°C.

different grades of PET were matched with different grades of EVOH, and the blends prepared are given in Table II.

Blend Morphology

Morphology of Blends After Extrusion

A representative fractograph of the as-cast PET/EVOH blend is shown in Figure 1. The general morphology of the blend is that of discontinuous EVOH spheres or ellipsoids in a continuous PET matrix. The aspect ratio of these domains is generally less than 1.2. A crazed fracture surface was evident in all as-cast blend fractographs.

Morphology of Blends After Biaxial Stretching

All blends clearly show an elliptical morphology. The long axis of the deformed EVOH particles in the micrographs lies in the plane of drawing. This implies that EVOH particles deform in the plane of the film during biaxial drawing. The extent of deformation can be characterized by the aspect ratio, which is defined as the length of the EVOH particles (major axis of ellipse) to the width (minor axis of ellipse) after drawing. Representative micrographs of blends stretched at 75, 80, 85, 90, and 110°C are given in Figures 2–6. Figures 7 and 8 give the dependence of aspect ratio with draw temperature for the uncompatibilized and compatibilized blends, respectively. Aspect ratio values have been averaged over 20 measurements. The general trend observed in all blends is that of a continuous decrease in aspect ratio with draw temperature within the allowance of the standard deviation.

Oxygen Permeability Results

Table IV presents measured oxygen permeability results for the blends used here. The results are plotted in Figures 9 and 10. Also given in Table IV and Figures 9 and 10 are the predictions of the Fricke model for permeability (see below).[15,20] With few exceptions, the general trend in the oxygen permeability is an increase with draw temperature. These data indicate that the aspect ratio of the platelets is important, where thinner (higher aspect ratio) particles are more effective in reducing the permeability than thicker (lower aspect ratio) particles.

Predicted Permeability Using the Fricke Model

The Fricke model was originally formulated to predict the electrical conductivity of a suspension of more permeable spheroids in a less permeable solution. It was assumed that the shorter axis of the spheroids was parallel to the direction of transport. The barrier properties of a homogeneous system, by analogy to Fricke's treatment of conductivity for a dispersion of nonconducting spheroids (ellipsoids, for this study) in a conducting matrix, is dealt with in Ref. 20. From the tabulated values and with the help of Figures 10 and 11, which give the measured and predicted OPVs for the blends processed at different draw temperatures, it can be seen that the model is more accurate (within 10%) in predicting the blend permeability at the higher draw temperatures. The measured and predicted permeability agree to a reasonable accuracy for high draw temperatures, but the measured values deviate increasingly negatively from the predicted values as the draw temperature is decreased.
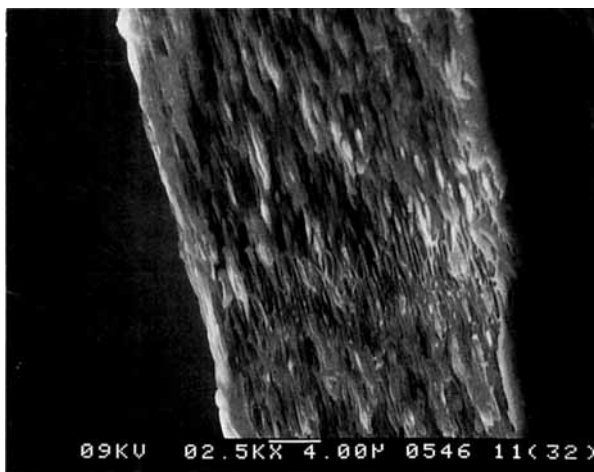

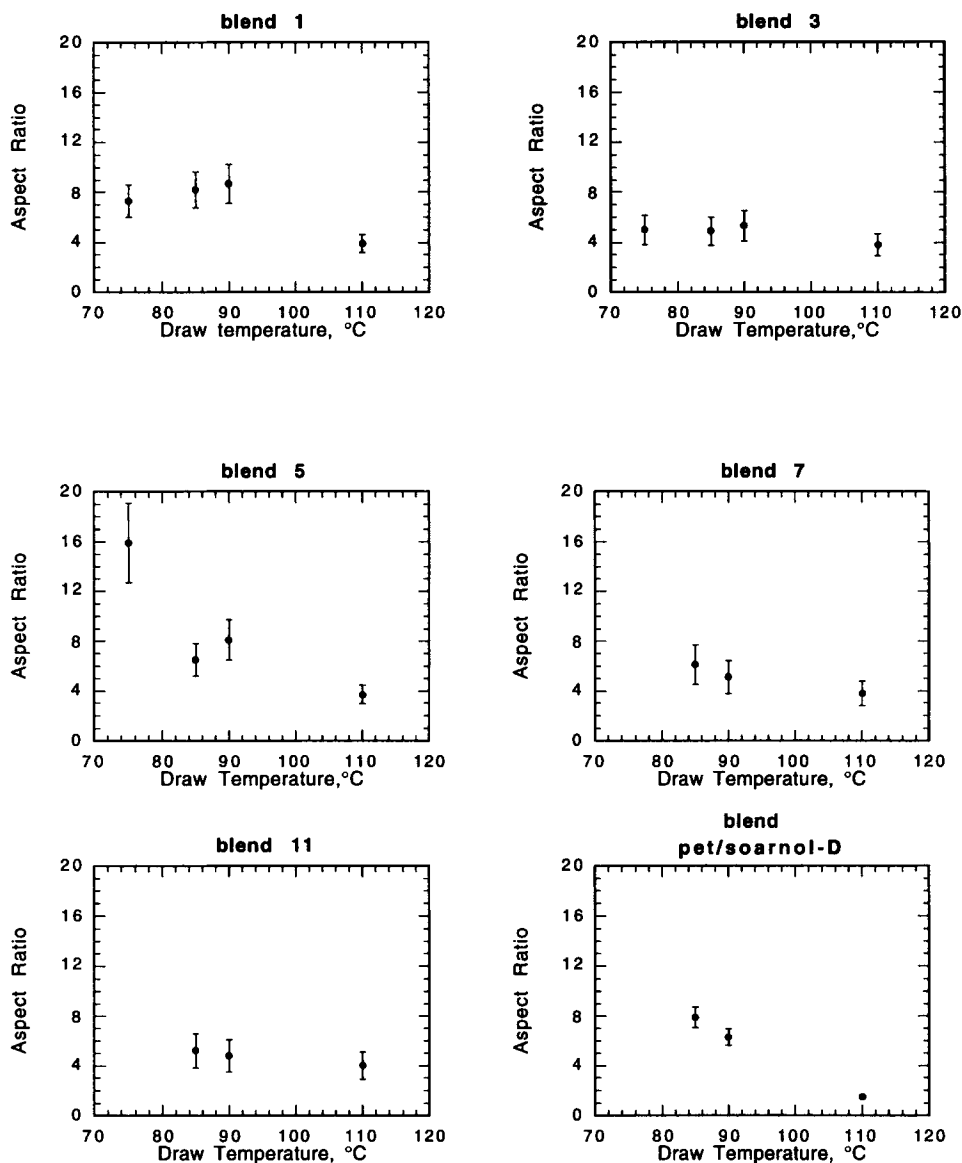**Figure 6** A representative fractograph of blends drawn at 110°C.

Figure 7   Aspect ratio of the uncompatibilized PET/EVOH blends processed at different draw temperatures.

DISCUSSION

Oxygen Permeability

It has been shown that the permeability of the blends increases with increasing draw temperature. This can be attributed to a decreasing aspect ratio of the EVOH particles with draw temperature. This creates a less tortuous path for the penetrant species, which is oxygen in this case. Also, the volume available for diffusion of the gaseous species is higher.

The aspect ratio of the EVOH particles is lower at high temperatures, since at these temperatures the matrix is less viscous as compared to the dispersed EVOH phase, as is evident from the table of flow stresses (Table III) and the match of PET and EVOH becomes poor. This implies that the amount of shear transferred to the EVOH particles is lower and the EVOH particles are deformed to a lesser degree. At lower temperatures, the flow stress of the matrix approaches more closely that of the dispersed phase. As a result, the load distribution between the matrix and the second phase is more uniform and the load transfer from the matrix to the EVOH phase is greater. Another factor for the low deformation in the EVOH phases could be that the interface between the PET and EVOH is weak and, hence, a transfer of stresses across the interface from the matrix to the dispersed particles is not very efficient.
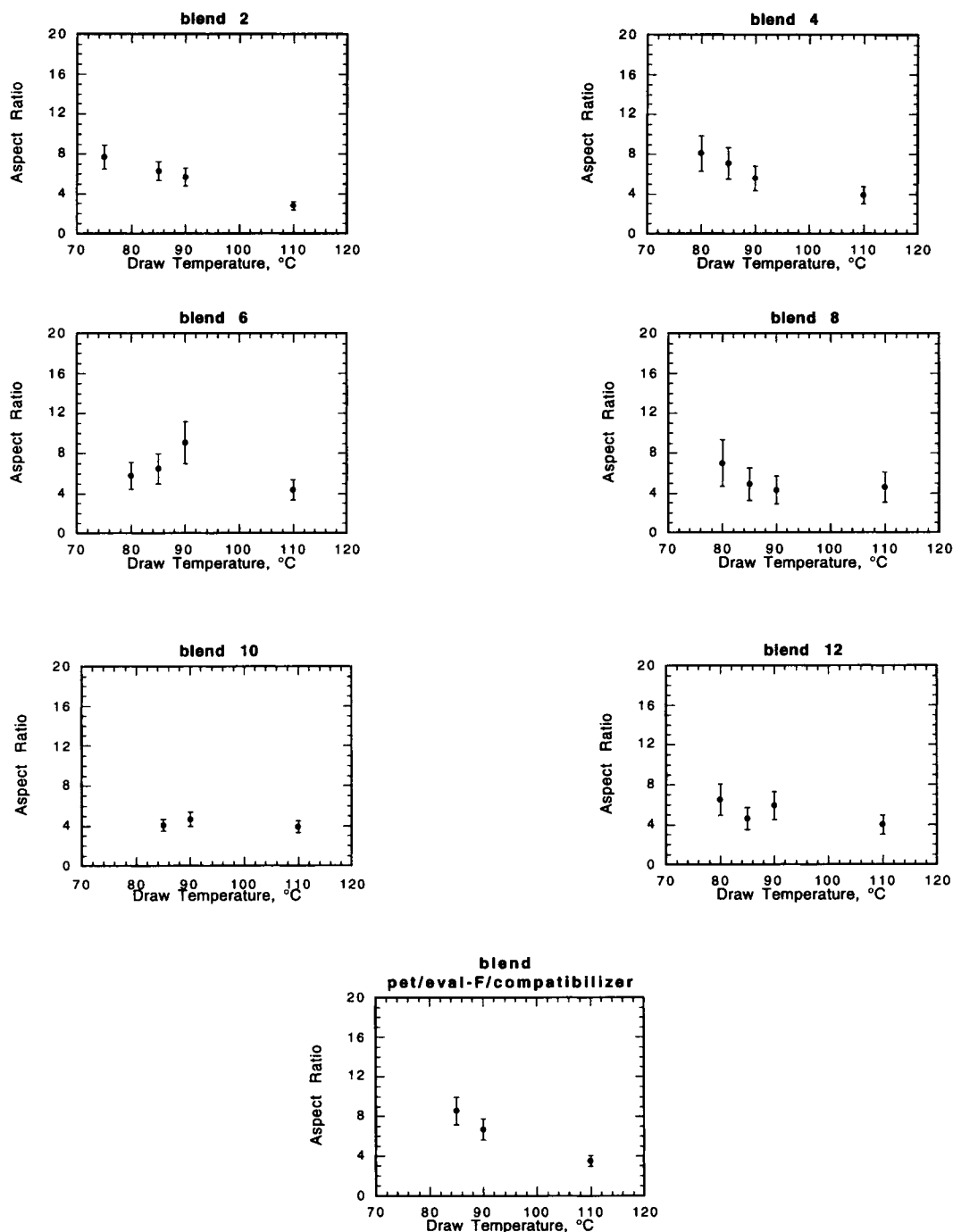
Figure 8   Aspect ratio of the compatibilized PET/EVOH blends processed at different draw temperatures.

The barrier efficiency of the blends can be evaluated by comparing their permeabilities to that expected for a laminate. The lowest measured permeability of the various blends made in this study and the predicted permeability of laminates with similar composition are given in Table V. It is clear that the permeability of the blends is higher than the predicted laminate permeability, by a factor as low as 1.1 for blends 1 and 2 to as high as 5.7 for the PET/Soarnol-D blend system.

Morphology Development

Morphology Development in the Extruder

The EVOH particles in the as-cast blends appear to be almost spherical. The spherical morphology is
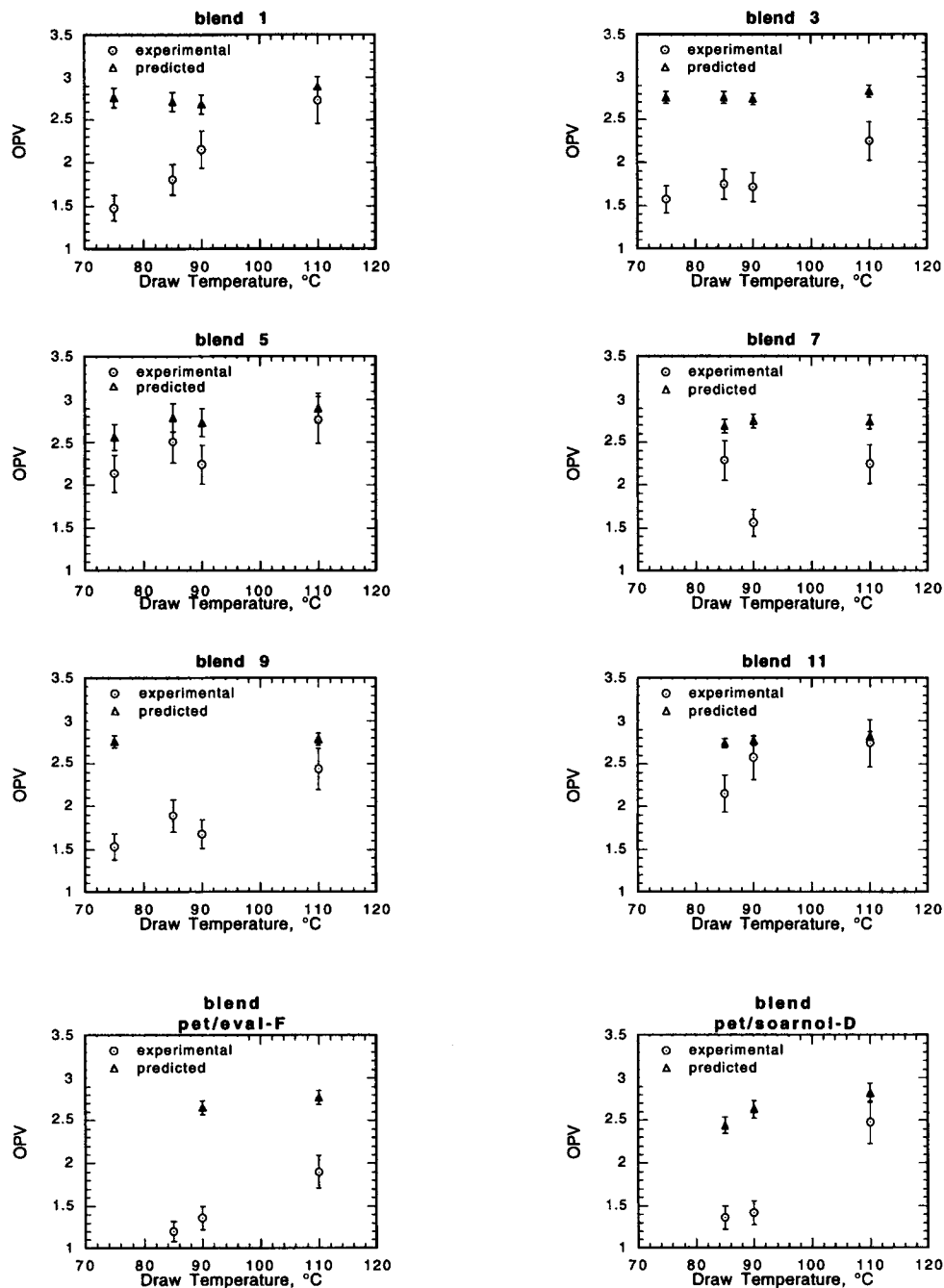
Figure 9 OPV of the uncompatibilized PET/EVOH blends processed at different draw temperatures.

consistent with the droplet breakup theory proposed by Tomatika[21] for Newtonian fluids. Droplet deformation involves the stretching of the drop, in a particular flow field, into a cylindrical body. This later breaks up into a line of droplets. Some blends, such as 9 and 10, show a small EVOH particle size in the as-cast condition. This could be due to a lower interfacial tension and a viscosity ratio closer to unity.[18]

Morphology Development by Biaxial Drawing

In drawn polymer blends, the dispersed particles in the matrix phase are deformed through biaxial stretching to platelets. It is seen that the EVOH phase in all the 3.5 × 3.5 drawn blends is in the form of platelets. These platelets can increase the path for the diffusing molecule (tortuosity).
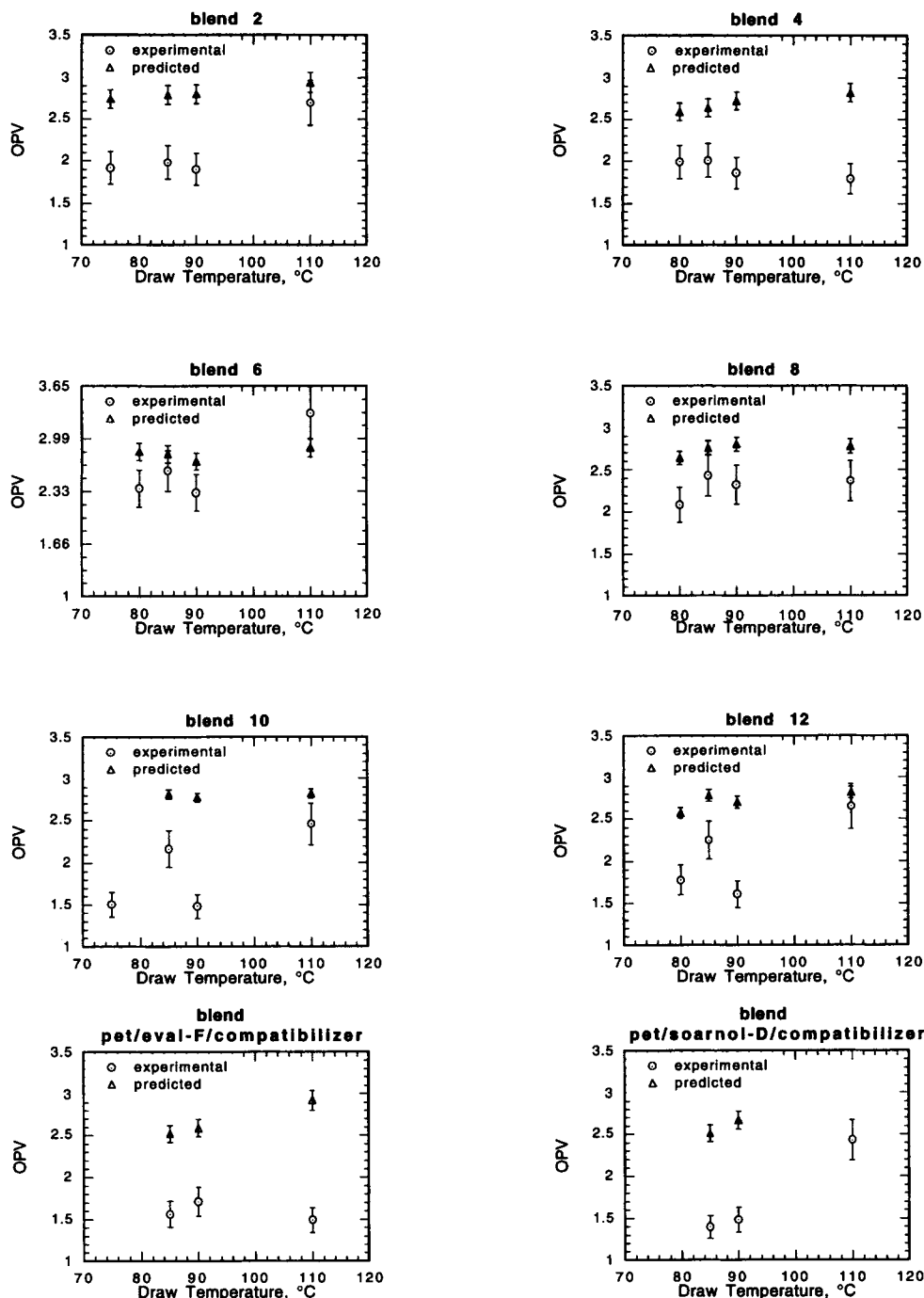
Figure 10   OPV of the compatibilized PET/EVOH blends processed at different draw temperatures.

The aspect ratio of these platelets is a function of the draw temperature, since at higher temperatures, the matrix is softer and therefore carries most of the load, while the EVOH particles remain considerably viscous. The shear on the EVOH particles is reduced, and, moreover, since the interfacial adhesion is poor,

they are deformed to a lesser degree. At the lower temperatures, the matrix has a viscosity comparable to that of the dispersed EVOH phase and the load is distributed more uniformly. Thus, both matrix and the dispersed phase deform adequately to carry the force applied due to stretching.

Table IV Predicted vs. Measured Permeability of the Blends at Different Processing Temperatures

No.	Blend PET/EVOH	Oxygen Permeability Value (OPV) (cc/mil/100 sq. in/24 h/atm)									
		Actual 75°C	Predicted 75°C	Actual 80°C	Predicted 80°C	Actual 85°C	Predicted 85°C	Actual 90°C	Predicted 90°C	Actual 110°C	Predicted 110°C
1	3974/4416	1.47	2.76	■	■	1.80	2.71	2.15	2.68	2.73	2.89
2	3974/4416 (c)	1.92	2.74	■	■	1.98	2.79	1.90	2.80	2.70	2.94
3	8257/3003	1.57	2.76	■	■	1.75	2.76	1.72	2.74	2.25	2.83
4	8257/3003 (c)	■	■	1.99	2.59	2.01	2.64	1.86	2.72	1.79	2.82
5	Shell/4416	2.13	2.56	■	■	2.50	2.79	2.24	2.73	2.76	2.90
6	Shell/4416 (c)	■	■	2.36	2.82	2.58	2.79	2.31	2.70	3.31	2.87
7	8202/3003	■	■	■	■	2.29	2.69	1.56	2.75	2.24	2.74
8	8202/3003 (c)	■	■	2.08	2.64	2.43	2.76	2.32	2.80	2.37	2.78
9	8257/BX230	1.53	2.76	■	■	1.89	≋	1.68	≋	2.44	2.79
10	8257/BX230 (c)	1.51	≋	■	■	2.17	2.81	1.48	2.77	2.46	2.82
11	8202/BX230	■	■	■	■	2.15	2.74	2.57	2.77	2.74	2.82
12	8202/BX230 (c)	■	■	1.78	2.57	2.25	2.78	1.61	2.70	2.65	2.82
	8307/E-F	■	■	■	■	1.20	≋	1.36	2.65	1.90	2.77
	8307/E-F (c)	■	■	■	■	1.56	2.52	1.72	2.59	1.49	2.92
	8307/Soarnol-D	■	■	■	■	1.36	2.44	1.42	2.63	2.48	2.82
	8307/Soarnol-D (c)	■	■	■	■	1.40	2.51	1.48	2.67	2.43	≋

(■) Stretching not done at this temperature. (≋) EVOH particles not seen in the micrograph.

Effect of the Compatibilizer on the Morphology

Evidence of a weak interface is found in the fractographs of the blends. Fracture occurred in all blends at the PET/EVOH interface. Further, the compatibilizer had no measurable effect on the EVOH particle size. Thus, the compatibilizer used in this work had no major effect on the morphological development and behavior.

EVOH has a similar structure to that of PE. The effect of the compatibilizer on the blends studied in this work is contrary to the findings of Carté and Moet[22] in their work with PET/PE blends using KRATON® FG-1901X as a compatibilizer. They observed a significant improvement in the mechanical properties of the PET/PE blend over that of pure PET.

Evaluation of Barrier Performance

Some theoretical approximations can be made with regard to estimating the barrier properties of the blends studied: As is seen in Table IV and Figures 9 and 10, the experimental values, in general, show the same trend as that of the theoretically predicted points, but the agreement improves with increasing draw temperature. There are two possible reasons for this. First, the degree of retained molecular orientation should be greater at lower draw temperatures, and Gohil[23,24] has shown that small molecule permeability decreases with molecular orientation in the amorphous phase in PET films. A second possibility is that the Fricke model may be accurate only at relatively low aspect ratios. In fact, the Fricke model has been experimentally validated only with

Table V Lowest Measured Permeability vs. Laminate Permeability for the Blends Prepared

Blend PET/EVOH	Predicted Laminate Permeability (cc/mil/100 sq in./day/atm)	Lowest Permeability Measured (cc/mil/100 sq in./day/atm)
3974/4416	1.35	1.47
8257/3003	0.62	1.57
Shell/4416	1.35	2.13
8202/3003	0.62	2.08
8257/BX230	0.62	1.48
8202/BX230	0.62	1.78
8307/Eval-F	0.26	1.20
8307/Soarnol-D	0.24	1.36

experimental data on the electrical conductivity of blood, which contains red corpuscles in the form of platelets (more precisely, biconcave) of aspect ratio 4.25. There is no experimental evidence evaluating the model at the higher aspect ratios of the present work.

CONCLUSIONS

The following conclusions derive from this study:

1. By rheologically matching the flow properties of the PET and EVOH grades, it is difficult to obtain blends with OPV of less than 1.
2. The copolymer used for compatibilization of the blends, SEBS (KRATON® FG-1901X), was not very successful in improving the interfacial adhesion or in creating a finer dispersion of the second phase in the blends.
3. All the blends studied have lower oxygen permeability than that of pure oriented PET. The greatest reduction in oxygen permeability was for the drawn uncompatibilized PET/EVAL-F blend stretched at 85°C, by a factor of 0.3 (OPV of oriented PET ~ 3.85 cc/mil/100 sq in./day/atm).
4. The Fricke model fails to quantitatively predict the dependence of permeability on EVOH aspect ratio for the blends used here.

REFERENCES

1. H. B. Hopfenberg and D. R. Paul, in *Polymer Blends*, D. R. Paul and S. Newman, Eds., Academic Press, New York, 1978, Vol. 1.
2. R. M. Gohil and J. Petermann, *J. Macromol. Sci. Phys. B*, **18**, 217 (1980).
3. R. M. Gohil and J. Petermann, *Colloid Polym. Sci.*, **260**, 312 (1982).
4. R. M. Gohil, *J. Polym. Sci. Phys. Ed.*, **23**, 1713 (1985).
5. R. Goddard, *Packag. Week*, **Oct.**, 21, 1993.
6. P. M. Subramanian, in *Barrier Polymers and Structures*, W. J. Koros, Ed., American Chemical Society, Washington, DC, 1990.
7. B. D. Favis, *J. Appl. Polym. Sci.*, **39**, 285 (1990).
8. K. Min, J. L. White, and J. F. Fellers, *Polym. Eng. Sci.*, **24**, 1327 (1984).
9. P. van Gheluwe, B. D. Favis, and J. P. Chalifoux, *J. Mater. Sci.*, **23**, 3910 (1988).
10. F. A. Shepherd, H. Gonzalez, and S. L. Hess, U.S. Pat. 4,835,214 (June 1, 1989).
11. Technical Bulletin No. 110, EVAL Company of America.
12. P. T. Delassus, *Tappi J.*, 217 (1988).
13. P. M. Subramanian and V. Mehra, in *ANTEC '86*, p. 301.
14. A. S. Michaels and R. B. Parker, Jr., *J. Polym. Sci.*, **41**, 53 (1959).
15. K. M. Kit, *Morphology and Barrier Properties of PET/EVOH and PEN/EVOH Blends*, to appear.
16. L. A. Utracki and B. D. Davis, in *Handbook of Polymer Science and Technology*, N. P. Cheremisinoff, Ed., Marcell Dekker, New York, 1989, Vol. 4.
17. G. N. Avgeropoulos, F. C. Weissert, P. H. Biddison, and G. C. A. Bohm, *Rubber Chem. Technol.*, **49**, 93 (1976).
18. S. Wu, *Polym. Eng. Sci.*, **27**, 335 (1987).
19. R. M. Gohil, *J. Appl. Polym. Sci.*, to appear.
20. H. Fricke, *Phys. Rev.*, **24**, 575 (1924).
21. S. Tomatika, *Proc. R. Soc. (Lond.) A*, **150**, 322 (1935).
22. T. L. Carté and A. Moet, *J. Appl. Polym. Sci.*, **48**, 611 (1993).
23. R. M. Gohil, *J. Appl. Polym. Sci.*, **28**(9), 1635 (1993).
24. R. M. Gohil, *J. Appl. Polym. Sci.*, **52**, 925 (1994).